Journal of Environmental Chemical Engineering 8 (2020) 103613

Contents lists available at ScienceDirect

Journal of Environmental Chemical Engineering

journal homepage: www.elsevier.com/locate/jece

Cerium oxide nanoparticles application for rapid adsorptive removal of tetracycline in water

Iis Nurhasanah*, Kadarisman, Vincensius Gunawan, Heri Sutanto

Department of Physics, Faculty of Science and Mathematics, Universitas Diponegoro Jalan Prof. Soedarto, S.H., Tembalang, Semarang, Central Java, 50275, Indonesia

ARTICLE INFO

Keywords:
CeO_2
Adsorption
Tetracycline
Water treatment

ABSTRACT

This study investigates the potential of CeO_2 nanoparticle as an adsorbent to remove tetracycline (TC) in water. CeO_2 nanoparticle was synthesized using precipitation method in water/alcohol mixed solvents. As-synthesized sample was characterized using x-ray diffractometer, scanning electron microscope, and Fourier transform infrared spectroscopy. The adsorption isotherm experiment was conducted in liquid phase by varying the contact time and the temperature at initial TC concentration of 25–125 mg/L. The result showed that CeO_2 has a cubic structure with crystallite size of 10.86 nm and is composed by aggregate particles. The equilibrium adsorption is reached after a contact time of 60 min that yield the removal efficiency of 80-97% and adsorption capacity of 58.03 mg/g. The adsorption kinetic analysis indicated that the adsorption process could be described by a pseudo second order model. The thermodynamic parameters confirmed that TC adsorption onto CeO_2 nanoparticle was exothermic and spontaneous. The high removal efficiency and short time adsorption equilibrium suggest that CeO_2 nanoparticle can be used as an antibiotic adsorbent for water treatment.

1. Introduction

Tetracycline (TC) is the second broad spectrum antibiotics largely used in human and veterinary medicine. Most TC used in medical treatment is poorly absorbed by humans or animals. Around 30 %–90 % of TC is excreted through urine and faeces as an active compound into the environment and becomes one of the emerging pollutants in water. Even though relatively low in concentration, the residue of TC in the aqueous environment leads to serious pollutant which contributes to increasing resistance of human pathogens, affecting human health and damaging ecosystem [1–3]. Therefore, the treatment method for TC removal in water is interesting to develop.

The waste water treatment method based on photodegradation [4–6], biocatalytic [7,8], Fenton-like process [9,10] and ultrasound irradiation [11,12] have been developed for TC removal in water. Among these methods, adsorption has been considered as an effective, economic and simple-operating method for removal of various water pollutants. Activated carbon is most intensively studied as effective adsorbent to remove antibiotic in water due to large surface area with microporous structure and high porosity [1–3]. Consequently, activated carbon showed superior adsorption capacity. However, the adsorption equilibrium of antibiotic onto activated carbon takes long time i.e in order of several to hundred hours [3]. In other report it is suggested to develop high performance of activated carbon preparation using feasible method from cheap raw materials to reduce cost production of activated carbon [1,2].

In recent years, a number of materials have been investigated as alternative adsorbents for TC removal [13–19]. CeO_2 is the most important rare earth metal oxide due to its wide range application including environmental [20,21], biomedical [22,23] and energy fields [24]. In term of water treatment application, CeO_2 is commonly used as a photocatalyst [25,26] and an adsorbent for removal of dye and heavy metal [27–31]. Furthermore, CeO_2 shows ability to degrade dyes by adsorpting/photodegradating simultaneously [32]. Even though CeO_2 nanoparticle has been considered as an excellent adsorbent for heavy metal and dyes removal, only few reports about CeO_2 application as an adsorbent for pharmaceutical removal are found. Brigante and Schultz showed the adsorption of minocycline on the CeO_2 is very fast in the initial several minutes [33,34]. Zhang et al. reported that the adsorption-desorption equilibrium of salicylic acid on the CeO_2-H_2O_2 system is reached after 40 min [35]. In addition, Guan et al. reported that catalytic activity of Co_3O_2/CeO_2 nanocomposite mediated with persulfate showed maximum TC degradation efficiency of 79% within 60 min [19]. Hence CeO_2 has the potential as an adsorbent to eliminate antibiotics in water quickly.

The adsorption properties of CeO_2 nanoparticle is influenced by

* Corresponding author.
E-mail address: nurhasanah@fisika.fsm.undip.ac.id (I. Nurhasanah).

https://doi.org/10.1016/j.jece.2019.103613
Received 13 September 2019; Received in revised form 28 November 2019; Accepted 15 December 2019
Available online 16 December 2019
2213-3437/

particle size as well as preparation method [31,32]. The high adsorption capacity of CeO_2 nanoparticle obtained using cerium (IV) sulphate precursor and cetyltrimethylammonium as a template in alkaline media due to smaller crystallite size than that CeO_2 nanoparticle prepared in acidic media [32]. In the previous report, we studied synthesis of CeO_2 nanoparticle using precipitation method in alkaline condition and calcined at various temperatures. The small crystallite size and good crystallinity of CeO_2 nanoparticle obtained at calcination temperature of 500 °C [23]. In this paper, we demonstrate the effectiveness of that CeO_2 nanoparticle as an adsorbent for TC removal in water. Precipitation is a simple method that can be utilized for large scale production of nanoparticle with low cost. CeO_2 nanoparticles were characterized by XRD, SEM, and FTIR techniques. The adsorption of TC onto CeO_2 nanoparticles was analysed using various adsorption models to determine kinetic parameters and adsorption mechanism. In addition, the effect of temperature on the adsorption of TC onto CeO_2 nanoparticle was studied to estimate the thermodynamic parameters.

2. Materials and methods

2.1. Materials

Cerium nitrate ($Ce(NO_3)_3.6H_2O$) as cerium precursor was purchased from Sigma-Aldrich Ltd. Ammonium hydroxide (Merck) was used as precipitant. Demineralized water (DW) and iso-propanol (Merck) were utilized as solvent. Tetracycline (TC) was obtained from pharmaceutical company in Indonesia.

2.2. Synthesis and characterization of CeO_2 nanoparticles

CeO_2 nanoparticle was synthesized by precipitation by following the procedures described previously [23]. Cerium nitrate solution (0.08 M) was made by dissolving cerium nitrate with mixed solvent of DW and iso-propanol. The solution was stirred by magnetic stirrer to obtain homogeneous solution. After that, ammonium hydroxide was added into the solution until pH 10 was reached. The precipitate was filtered and washed with ethanol several times, then dried at 100 °C for 3 h. The dried precipitate was finally calcined at 500 °C for 2 h to form crystalline of CeO_2 nanoparticles. X-ray diffractometer (PANalytical), scanning electron microscope (JEOL JSM 6360) and Fourier transform infrared spectroscopy were used to characterize structure, morphology and functional group of CeO_2 nanoparticles respectively. The average crystal size of CeO_2nanoparticle was calculated using Scherer formula:

$$D = \frac{0.9\lambda}{\beta\cos\theta}, \tag{1}$$

where D represents crystallite size, λ is wavelength of x-ray, β denotes FWHM and θ is diffraction angle.

2.3. Adsorption experiment

The adsorption isotherm experiment of TC was carried out at initial concentration in the range 25–125 mg/L. Sample with 15 mg nanoparticles CeO_2 was added to 10 mL TC solution. The mixture was stirred with the speed rotation of 300 rpm in the dark condition at different temperature (303 K, 313 K and 323 K). Experiment was performed at natural condition of TC solution. The sample was taken in interval time of 15 − 120 min and centrifuged at 6000 rpm for 10 min to separate adsorbent from solution. The residual of TC concentration was analysed by UV–vis spectrophotometer (UV Vis 1240 Shimadzu) at 356 nm. The removal efficiency and the adsorption capacity of CeO_2 nanoparticles were calculated using the following equations:

$$RE\ (\%) = \frac{(C_o - C_e)}{C_o} \times 100 \tag{2}$$

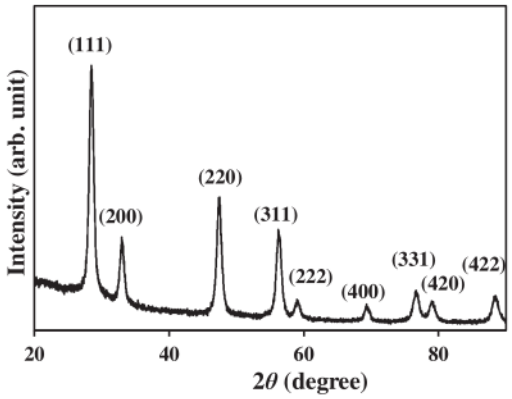

Fig. 1. The XRD pattern of CeO_2 nanoparticles.

$$q_t = \frac{(C_o - C_t)V}{m} \tag{3}$$

where RE (%) and q_t (mg/g) are adsorptive removal efficiency and adsorption capacity, C_o (mg/L) and C_t (mg/L) represent the initial concentration and concentration of TC at contact time (t), V is volume of TC solution (L), and m (g) denotes the weight of CeO_2 nanoparticle.

3. Results and discussion

3.1. Properties of CeO_2 nanoparticles

The structure of CeO_2 was analysed using XRD with the results illustrated in Fig.1. In that figure, the diffraction peaks were shown at 2θ = 28.43°; 32.97°; 47.52°; 56.37°; 59.10°; 69.29°; 76.51°; 78.98° and 88.20°. These peaks were corresponded to the plane: (111), (200), (220), (311), (222), (400), (331), (420) and (422) for face centre cubic (fcc) structure in XRD standard pattern for CeO_2 (JCPDS No. 43-0394).

The XRD pattern did not show diffraction peaks which was associated to the other phase. This indicated a single phase of CeO_2 [21,25,32]. The high and sharp diffraction peaks designated CeO_2 had a good crystallinity. The average crystal size was 10.68 nm which is obtained based on full width at half-maximum (FWHM) of (111) plane and using Scherer formula (Eq. (1)).

The SEM image in Fig. 2a shows that CeO_2 consists of particles in the sphere-like form. It seems that particles interconnected each other to form aggregates. This is possible since coagulation occurs when the precipitation process is taking place in the medium base. The appearance of the aggregates is similar to CeO_2 nanoparticles which is synthesised using sol gel [25], precipitation [26], and hydrothermal method [30].

FTIR spectroscopy is employed to identify functional group and also atomic and molecule vibration. Functional group is one of the many factors which affects adsorption efficiency. In Fig. 2b, FTIR spectrum shows several absorption peaks in the interval of wavelength of 400 cm^{-1} to 4000 cm^{-1}. The spectrum band is wide, around 3413 cm^{-1} which is associated with the stretching vibration of O−H. The absorption band at 1542 cm^{-1} and 1342 cm^{-1} is related to OH-adopted water molecule. An absorption peak at 492 cm^{-1} which is associated to the vibration of Ce-O indicates formation of pure CeO_2 phase as it is observed by XRD analysis [21,26,32].

3.2. Adsorption TC on CeO_2 nanoparticles

Fig. 3 shows TC removal efficiency and adsorption capacity of CeO_2 nanoparticles versus contact time for various initial TC concentrations at temperature of 303 K. It seems that the removal efficiency more than

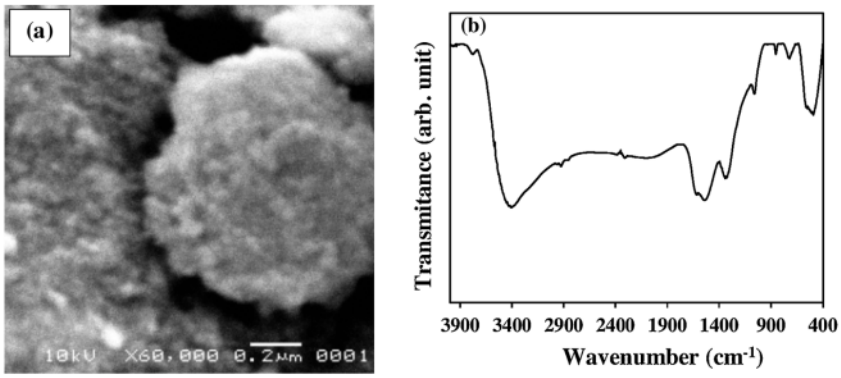

Fig. 2. (a) SEM image of nanoparticle CeO_2 and (b) FTIR spectrum of nanoparticle CeO_2.

60% was obtained within the first 15 min contact time for initial TC concentration 25 mg/L to 100 mg/L and around 80–96% of TC was removed within 60 min. As a comparison, the removal efficiency of 50% TC (40 mg/L) occurred within 60 min using MgO nanoparticle [36] and 96% using MOF-5 [16]. On other report, removal efficiency of 86 % TC (10 mg/L) was observed within 60 min using MgO-loaded SiO_2 nanocomposite [15], while removal efficiency of 20 mg/L TC was 70–88 % using activated carbon with agitation time of 24 h [37]. Likewise, the adsorption capacity increased as the contact time and the initial TC concentration increased up to 100 mg/L and decreased at the initial TC concentration of 125 mg/L. Rapid adsorption occurred in the first 15 min of contact time. In this interval time, the rate of TC adsorption was high indicating that the high amounts of active sites existed at the surfaces of nanoparticle CeO_2. After 15 min contact time, the adsorbed TC on CeO_2 nanoparticle increased slightly until 60 min. The adsorption process was extended to 120 min to ensure the equilibrium condition is achieved. Then after 60 min, the rate of adsorption decreased. It is showed that in the interval of contact time from 60 min to 120 min, TC is difficult to be adsorbed onto CeO_2 nanoparticle due to repulsive force between TC molecules. Hence, we concluded that 60 min was a required time to achieve equilibrium condition. This was faster compare to the time to achieve equilibrium state for activated carbon (8 h) [37], CU-immobilized alginate (24 h) [17], porous carbon (8 h for TC concentration of 25 – 45 mg/L and 24 h for high TC concentration) [38], and graphene oxide (90 min) [18] in TC adsorption process.

The removal efficiency and adsorption capacity versus initial TC concentration were summarized in Fig. 4(c). The removal of TC decreased slightly when the concentration increased from 25 mg/L to 100 mg/L, then decreased sharply at concentration of 125 mg/L. The high removal efficiency of 80–97% showed that CeO_2 nanoparticle can be used as an effective adsorbent for TC removal with concentration up to 100 mg/L. On the other hand, adsorption capacity increased with enhanced TC concentration. The maximum adsorption capacity of CeO_2

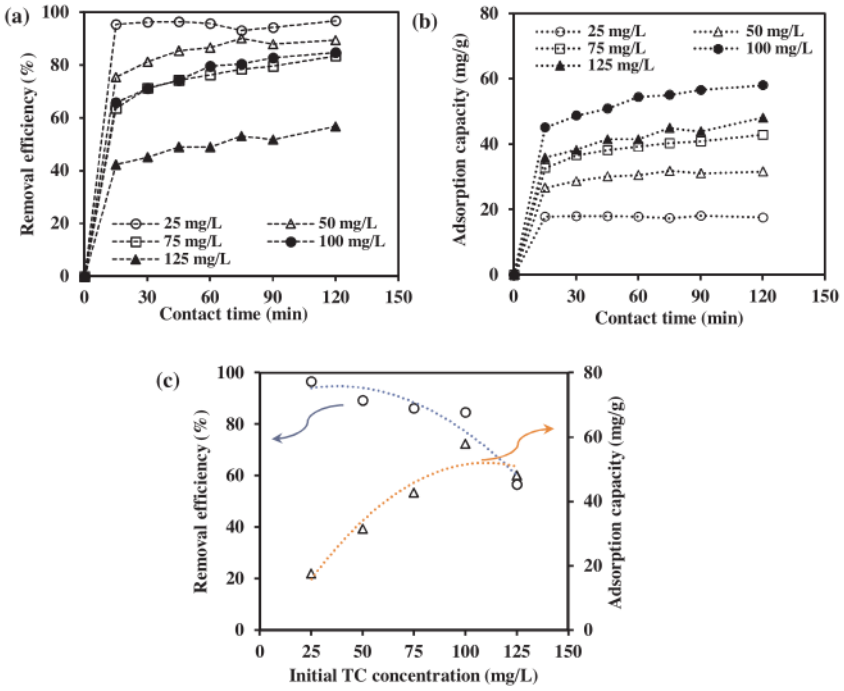

Fig. 3. (a) Removal efficiency, (b) Adsorption capacity versus contact time and (c) Removal efficiency and adsorption capacity versus initial TC concentration.

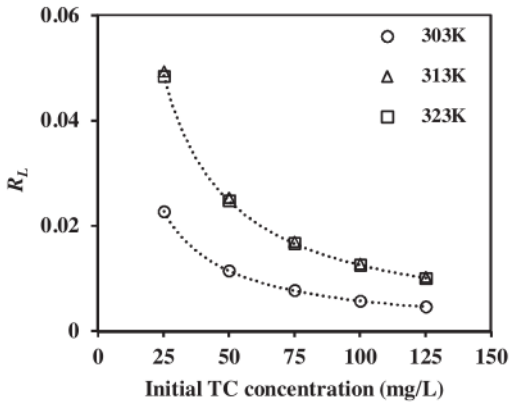

Fig. 4. Langmuir separation factor versus initial TC concentration.

nanoparticles for TC adsorption was 58.03 mg/g for initial TC concentration of 100 mg/L. Although, those value was smaller than TC adsorption capacity of activated carbon but this result was comparable with TC adsorption capacity of CU-immobilized alginate i.e 5326 mg/g at initial TC concentration of 90 mg/L [17]. This finding implies that the adsorptive removal performance of our CeO_2 nanoparticle is higher than other adsorbent as reported in literature [15,36,37].

To analyse the adsorption mechanism, the experimental data of TC onto CeO_2 nanoparticle at 303 K, 313 K and 323 K were fitted using three isotherm models i.e Langmuir, Freundlich and Temkin [18]. The highest correlation coefficient (R^2) was obtained for data fitting by the Langmuir model. The linear equation of Langmuir model is given by Eq. (4).

$$\frac{1}{q_e} = \frac{1}{q_m} + \frac{1}{K_L q_m C_e} \tag{4}$$

where q_m (mg/g) is the maximum adsorption capacity, K_L (L/mg) is the Langmuir isotherm constant. Therefore, TC adsorption onto CeO_2 nanoparticle was more appropriate described by the Langmuir model than Freundlich and Temkin model. This result is in accordance with tetracycline adsorption on other adsorbent i.e porous carbon [38], graphene oxide [18] and dyes adsorption onto CeO_2 nanoparticle [31]. The Langmuir isotherm model assumes the equivalent and uniform adsorption site exist on the adsorbent surface where the adsorbate molecule did not interact to each other. The maximum adsorption is achieved when the adsorbate covers the entire adsorbent surface completely formed monolayer [14,16,39,40]. The adsorption isotherm parameters of TC onto CeO_2 nanoparticles based on Langmuir model were listed in Table 1. The high R^2 obtained at adsorption temperature of 303 and 313 K showed that TC adsorption onto CeO_2 nanoparticle was monolayer adsorption on homogeneous adsorbent surface [16,38]. The maximum monolayer adsorption capacity increased from 46.51 mg/g to 57.14 mg/g when the temperature raised from 303 to 313 K. Then, the maximum monolayer adsorption capacity decreased to 52.36 mg/g when the temperature as high as 323 K which could be associated to the water evaporation of TC solution [15]. Therefore, the TC adsorption onto CeO_2 is more favourable at moderate temperature.

The nature of Langmuir model of TC adsorption onto CeO_2 nanoparticle can be determined using the value of Langmuir separation factor (R_L) as described by equation (5). Langmuir separation factor is essential isotherm characteristic. The value of this separation factor determines the nature of adsorption process. The process is linear ($R_L = 1$) or irreversible ($R_L = 0$) or unfavourable ($R_L > 1$) or favourable ($R_L < 1$) which is calculated by

$$R_L = \frac{1}{1 + K_L C_o} \tag{5}$$

Fig. 4 shows the Langmuir separation factor versus initial TC concentration at adsorption temperature of 303, 313 and 323 K. It can be seen that R_L values for different TC concentration and different temperature were smaller than 1. This result confirms that adsorption TC onto CeO_2 nanoparticle was favourable.

The effect of contact time on the TC adsorption onto CeO_2 nanoparticle was used to analyse adsorption kinetics. The adsorption kinetic determines the mechanism and parameters of adsorption which is important to realize the practical application of CeO_2 nanoparticle adsorbent. Several adsorption kinetic models have been used for representing TC adsorption onto various adsorbents. These models are: pseudo-first-order, pseudo-second-order and intra-particle diffusion [16,17,38]. The kinetic of adsorption for pseudo-first-order model is given by

$$\log(q_e - q_t) = \log q_e - \frac{k_1}{2.303} t, \tag{6}$$

where q_e and q_t represent the amount of adsorbate (mg g^{-1}) in equilibrium condition and in certain time t, respectively while k_1 is the rate of adsorption (min^{-1}).

In pseudo second order model, the rate of adsorption is determined as

$$\frac{t}{q_t} = \frac{1}{k_2 q_e^2} + \frac{1}{q_e} t \tag{7}$$

where k_2 is the adsorption rate constant of pseudo second order (g mg^{-1} min^{-1}). The slope and intercept of the curve t/q_t against t is used to calculate a constant k_2.

The third model, based on intra-particle diffusion (Weber-Morris), is formulated as:

$$q_t = k_p t^{1/2} + C, \tag{8}$$

where k_p represents the constant of diffusion intra-particles rate (mg g^{-1} $min^{1/2}$) and C is the thickness of boundary layer. The k_p and C can be obtained from the slope and intercept of linear curve q_t against $t^{1/2}$.

The fitting of the experiment data using pseudo first-order kinetic model yields poor linearity with the small correlation coefficient value ($R^2 < 0.9$). It indicated that the TC adsorption onto CeO_2 nanoparticle did not dominated by physical adsorption [17]. The experimental data fitted well to both other models (pseudo-second order and intra-particle diffusion) with the high $R^2 > 0.9$. The fitting of experiment data using the adsorption kinetic models of pseudo-second order and intra-particle diffusion was depicted in Fig. 5. Parameters for each kinetic model are summarized in Table 2. The highest R^2 obtained for pseudo-second order model and the theoretical values of q_e for all concentration TC are close to the experimental values. The rate adsorption (k_2) constants were found to be 0.187 to 0.472 g/mg min which much higher than TC adsorption on graphene oxide i.e 0.104×10^{-3} g/mg min [14], 0.065 g/mg h [18], and activated carbon (2.7×10^{-4} g/mg h) [38].

In order to analyse effect of the rate controlling step in the TC adsorption, the intraparticle diffusion plot was used for fitting experiment data. Fig. 5(b) shows two stages of linear relationship. Rapid adsorption at the initial contact time resulted in line passed through the origin which confirmed that intraparticle diffusion in TC adsorption was the rate-controlling step. In this stage, the main factor affecting the adsorption process is outer surface adsorption. The second line did not pass through the origin, the intercept (C) increased as the TC

Table 1
Adsorption Isotherm Parameters of Langmuir Model.

T (K)	q_m (mg/g)	K_L(L/mg)	R^2
303	46.51	1.72	0.9352
313	57.14	0.81	0.9780
323	52.36	0.79	0.7900

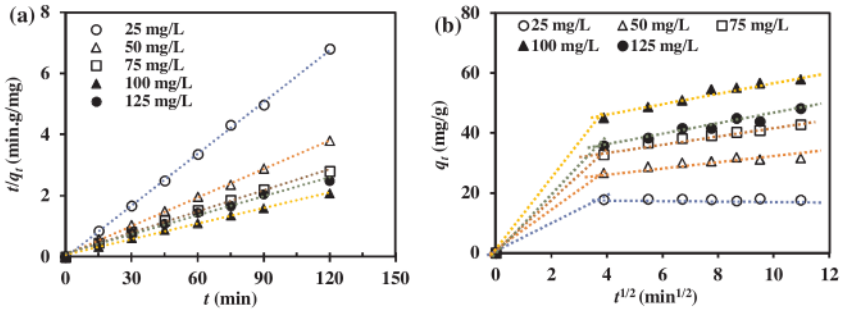

Fig. 5. Adsorption kinetic model (a) pseudo-second order, and (b) intra-particle diffusion.

Table 2
Parameters of adsorption kinetic of Tetracycline onto nanoparticles CeO_2.

Model	Parameter	TC concentration (mg/L)			
		50	75	100	125
Pseudo second order	$q_{e,exp}$ (mg/g)	31.63	42.88	58.02	48.16
	$q_{e,cal}$ (mg/g)	32.05	43.10	58.82	48.08
	k_2 (g/mg min)	0.472	0.242	0.235	0.187
	R^2	0.9990	0.9966	0.9966	0.9917
Intraparticle diffusion	$q_{e,exp}$ (mg/g)	31.63	42.88	58.02	48.16
	$q_{e,cal}$ (mg/g)	32.49	43.26	59.13	47.72
	k_p (mg/g $min^{1/2}$)	0.7009	1.3405	1.8878	1.6635
	C (mg/g)	24.811	28.574	38.449	29.492
	R^2	0.8453	0.964	0.9701	0.9528

concentration increased up to 100 mg/L. The C value suggested that the intra-particle diffusion was not only controlled by the rate-controlling step but also controlled by boundary layer. Therefore, the TC adsorption onto CeO_2 nanoparticle was suitable described by pseudo-second order kinetic model, and confirmed that adsorption process was homogeneous and controlled by chemisorption [33,39]. This finding is similar to the previous study that used other adsorbent [16–19].

The effect of temperature on the equilibrium adsorption capacity of TC adsorption onto CeO_2 nanoparticle was investigated at temperature of 303, 313 and 323 K. As shown in Fig. 6, the temperature dependence of the amount of TC adsorbed on the CeO_2 nanoparticle for different initial TC concentration was irregular in nature. There was slightly increased in the amount of TC adsorbed on the CeO_2 nanoparticle with increasing temperature for low TC concentration of 25 mg/L and 50 mg/L. However, the amount of TC adsorbed on CeO_2 nanoparticle for initial TC concentration of 75, 100 and 125 mg/L increased firstly from 303 K to 313 K and then decreased with increasing temperature at 323 K.

Based on the experiment data of TC adsorption at different temperature, the thermodynamic parameters were studied to determine the

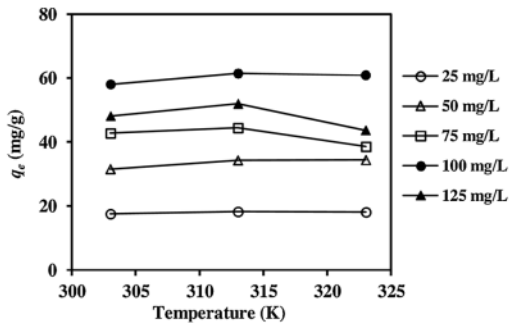

Fig. 6. Adsorption capacity of TC for different concentration and temperature.

Table 3
Change of thermodynamic parameters with temperature.

Thermodynamic parameter				
ΔH (kJ/mol)	ΔS (J/mol)	ΔG (kJ/mol)		
		303 K	313 K	323 K
−27.23	−54.01	−11.038	−9.956	−9.982

nature of adsorption process whether physical or chemical, endothermic or exothermic, spontaneous or nonspontaneous. Table 3 displays the thermodynamic parameters including Gibbs' free energy change (ΔG), enthalpy change (ΔH) and entropy change (ΔS) which were obtained using equations as [17]:

$$\Delta G = -RT\ln K_d \tag{9}$$

$$\ln K_d = \frac{\Delta S}{R} - \frac{\Delta H}{RT} \tag{10}$$

Here, parameters R and T refer to the gas constant (8.314 J/mol K) and absolute temperature (K), respectively. K_d is equilibrium constant equals to $q_m k_L$ (L/mg). The value of ΔH and ΔS were obtained from the slope and intercept of the graph of Ln K_d versus $1/T$, while the value of ΔG was calculated at 303, 313 and 323 K using equation (9).

The negative of ΔG in the range temperature of 303 − 323 K represented that TC adsorption was feasible and spontaneous process. The increasing of ΔG value as the temperature increases indicated that adsorption is more feasible and spontaneous at lower temperature. The negative value of ΔH revealed that TC adsorption was exothermic process. These results are different from adsorption of minocycline onto CeO_2 nanoparticle [33]. Therefore, the nature of adsorption property of CeO_2 nanoparticle depend on the type of antibiotic. Moreover, the negative of ΔS confirmed that randomness at the liquid-solid interface was reduced as well as the affinity of adsorbent for adsorption. The negative or positive values of ΔH and ΔS were depended on initial TC concentration. Both negative values of ΔH and ΔS were found for TC adsorption onto activated carbon at initial concentration below 200 mg/L [13,41], otherwise the positive value of ΔH and ΔS observed for initial concentration higher than 200 mg/L [41]. The initial TC concentration in this study is lower than 200 mg/L, therefore our result consistent with the result that reported previously [13,41].

Our study showed that, CeO_2 nanoparticle has excellent adsorption performance for TC removal in water. CeO_2 nanoparticle possesses high removal efficiency and high rate adsorption constant. The rapid antibiotics removal, as well as inexpensive preparation methods of CeO_2 nanoparticle are very beneficial for practical application.

4. Conclusion

The CeO_2 nanoparticle had the potential as an adsorbent for rapid removal of TC in water. The high removal efficiency of 96% was achieved within 15 min of contact time. The TC adsorption onto CeO_2

nanoparticles followed the Langmuir isotherm and the pseudo-second order kinetic model. The thermodynamic study indicated that TC adsorption was exothermic and spontaneous. The fast and high removal efficiency of TC suggested that CeO_2 nanoparticle have the opportunity to be used for pharmaceutical wastewater treatment.

Author contributions

Author 1: Iis Nurhasanah
Conceived and designed the analysis
Collected the data
Contributed data or analysis tools
Performed the analysis
Wrote the paper
Author 2: Kadarisman
Collected the data
Contributed data or analysis tools
Author 3: Vincensius Gunawan
Performed the analysis
Wrote the paper
Author 4: Heri Sutanto
Performed the analysis

Declaration of Competing Interest

Authors have declared that no conflict of interest exists in this publication.

Acknowledgments

We acknowledge The Ministry of Research, Technology and Higher Education of Indonesia for full funding of this research with contract number: No. 125/SP2H/ PTNBH/DRPM/2019.

References

[1] F. Yu, Y. Li, S. Han, J. Ma, Adsorptive removal of antibiotics from aqueous solution using carbon materials, Chemosphere 153 (2016) 365–585, https://doi.org/10.1016/j.chemosphere.2016.03.083.
[2] X. Zhang, W. Guo, H.H. Ngo, H. Wen, N. Li, W. Wu, Performance evaluation of powdered activated carbon for removing 28 types of antibiotics from water, J. Environ. Manage. 172 (2016) 193–200, https://doi.org/10.1016/j.jenvman.2016.02.038.
[3] M.J. Ahmed, Adsorption of quinolone, tetracycline, and penicillin antibiotics from aqueous solution using activated carbons: review, Environ. Toxicol. Pharmacol. 50 (2017) 1–10, https://doi.org/10.1016/j.etap.2017.01.004.
[4] J. Lyu, Z. Hu, Z. Li, M. Ge, Removal of tetracycline by BiOBr microspheres with oxygen vacancies: combination of adsorption and photocatalysis, J. Phys. Chem. Solids 129 (2019) 61–70, https://doi.org/10.1016/j.jpcs.2018.12.041.
[5] P. Demircivi, E.B. Simsek, Visible-light-enhanced photoactivity of perovskite-type W-doped $BaTiO_3$ photocatalyst for photodegradation of tetracycline, J. Alloys. Compd. 774 (2019) 795–802, https://doi.org/10.1016/j.jallcom.2018.09.354.
[6] N. Belhouchet, B. Hamdi, H. Chenchouni, Y. Bessekhouad, Photocatalytic degradation of tetracycline antibiotic using new calcite/titania nanocomposites, J. Photochem. Photobiol. A: Chem. 372 (2019) 196–205, https://doi.org/10.1016/j.jphotochem.2018.12.016.
[7] S. Shao, Y. Hu, J. Cheng, Y. Chen, Biodegradation mechanism of tetracycline (TEC) by strain Klebsiella sp. SQY5 as revealed through products analysis and genomics, Ecotoxicol. Environ. Safety 185 (2019) 109676, , https://doi.org/10.1016/j.ecoenv.2019.109676.
[8] X. Liao, R. Zou, B. Li, T. Tong, S. Xie, B. Yuan, Biodegradation of chlortetracycline by acclimated microbiota, Pro.Safe Environ. Protect. 109 (2017) 11–17, https://doi.org/10.1016/j.psep.2017.03.015.
[9] M. Khodadadi, A.H. Panahi, T.J. Al-Musawi, M.H. Ehrampoush, A.H. Mahvi, The catalytic activity of $FeNi_3$@SiO_2 magnetic nanoparticles for the degradation of tetracycline in the heterogeneous Fenton-like treatment method, J. Water Process Eng. 32 (2019) 100943, , https://doi.org/10.1016/j.jwpe.2019.100943.
[10] N. Zhang, J. Chen, Z. Fang, E.P. Tsang, Ceria accelerated nanoscale zerovalent iron assisted heterogeneous Fenton oxidation of tetracycline, Chem. Eng. J. 369 (2019) 588–599, https://doi.org/10.1016/j.cej.2019.03.112.
[11] R.D.C. Soltani, M. Mashayekhi, M. Naderi, G. Boezkaj, S. Jorfi, M. Safari, Sonocatalytic degradation of tetracycline antibiotic using zinc oxide nanostructures loaded on nano-cellulose from waste straw as nanosonocatalyst, Ultrason. Sonochem. 55 (2019) 117–124, https://doi.org/10.1016/j.ultsonch.2019.03.009.
[12] S. Nasseri, A.H. Mahvi, M. Seyedsalehi, K. Yaghmaeian, R. Nabizadeh, M. Alimohammadi, G.H. Safari, Degradation kinetics of tetracycline in aqueous solutions using peroxydisulfate activated by ultrasound irradiation: effect of radical scavenger and water matrix, J. Mol. Liq. 241 (2017) 704–714, https://doi.org/10.1016/j.molliq.2017.05.137.
[13] J. Ma, Y. Lei, M.A. Khan, F. Wang, Y. Chu, W. Lei, M. Xia, S. Zhu, Adsorption properties, kinetics & thermodynamics of tetracycline on carboxymethyl-chitosan reformed montmorillonite, Inter. J. Bio. Mac. 124 (2019) 557–567, https://doi.org/10.1016/j.ijbiomac.2018.11.235.
[14] J. Miao, F. Wang, Y. Chen, Y. Zhu, Zhou Y, S. Zhang, The adsorption performance of tetracyclines on magnetic graphene oxide: a novel antibiotics absorbent, Appl. Ssurf. Sci. 475 (2019) 549–558, https://doi.org/10.1016/j.apsusc.2019.01.036.
[15] Y. Yue, Z. Peng, W. Wang, Y. Cai, F. Tan, X. Wang, X. Qiao, Facile preparation of MgO-Loaded SiO_2 nanocomposites for tetracycline removal from aqueous solution, Powder Technol. 347 (2019) 1–9, https://doi.org/10.1016/j.powtec.2019.02.034.
[16] S.M. Mirsoleimani-azizi, P. Setoodeh, S. Zeinali, M.R. Rahimpour, Tetracycline antibiotic removal from aqueous solutions by MOF-5: adsorption isotherm, kinetic and thermodynamic studies, J. Environ. Chem. Eng. 6 (2018) 6118–6130, https://doi.org/10.1016/j.jece.2018.09.017.
[17] X. Zhang, X. Lin, Y. He, Y. Chen, X. Luo, R. Shang, Study on adsorption of tetracycline by Cu-immobilized alginate adsorbent from water environment, Inter. J. Biol. Macromol. 124 (2019) 418–428, https://doi.org/10.1016/j.ijbiomac.2018.11.218.
[18] Y. Gao, L. Zhang, H. Huang, J. Hu, S.M. Shah, X. Su, Adsorption and removal of tetracycline antibiotics from aqueous solution by graphene oxide, J. Colloid Interface Sci. 368 (2012) 540–546, https://doi.org/10.1016/j.jcis.2011.11.015.
[19] R. Guan, X. Yuan, Z. Wu, L. Jiang, J. Zhang, Y. Li, G. Zeng, D. Mo, Efficient degradation of tetracycline by heterogeneous cobalt oxide/cerium oxide composites mediated with persulfate, Sep. Purif. Technol. 212 (2019) 223–232, https://doi.org/10.1016/j.seppur.2018.11.019.
[20] M.S. Hasan, R. Khan, T. Amna, J. Yang, I.H. Lee, M.Y. Sun, M.H. El-Newethy, S.S. Al-Deyab, M.S. Khil, The influence of synthesis method on size and toxicity of CeO_2quantum dots: Potential in environmental remediation, Ceram. Int. 42 (2016) 576–582, https://doi.org/10.1016/j.ceramint.2015.08.149.
[21] A. Umar, R. Kumar, M.S. Akhtar, G. Kumar, S.H. Kim, Growth and properties of well-crystalline cerium oxide (CeO_2) nanoflakes for environmental and sensor applications, J. Colloid Interface Sci. 454 (2015) 61–68, https://doi.org/10.1016/j.jcis.2015.04.055.
[22] H.E. Liying, S.U. Yumin, J. Lanhong, S.H.I. Shikao, Recent advances of cerium oxide nanoparticles in synthesis, luminescence and biomedical studies: a review, J. Rare Earth 33 (8) (2015) 791–799, https://doi.org/10.1016/S1002-0721(14)60486-5.
[23] I. Nurhasanah, W. Safitri, T. Windarti, A. Subagio, The calcination temperature effect on the antioxidant and radioprotection propertis of CeO_2 nanoparticles, Reaktor 18 (1) (2018) 22–26, https://doi.org/10.14710/reaktor.18.1.22-26.
[24] M. Melchionna, P. Fornasiero, The role of ceria-based nanostructured materials in energy applications, Mater. Today 17 (7) (2014) 349–357 https://doi.org/10.1016/j.mattod.2014.05.005.
[25] L. Nadjia, E. Abdelkader, B. Naceur, B. Ahmed, CeO_2 nanoscale particles: synthesis, characterization and photocatalytic activity under UVA light irradiation, J. Rare Earth 36 (2018) 575–587, https://doi.org/10.1016/j.jre.2018.01.004.
[26] P.K. Sane, S. Tambat, S. Sontakke, P. Nemade, Visible light removal of reactive dyes using CeO_2 synthesized by precipitation, J. Environ. Chem. Eng. 644 (2018) 4476–4489, https://doi.org/10.1016/j.jece.2018.06.046.
[27] H. Wang, Y. Zhong, H. Yu, P. Aprea, S. Hao, High-efficiency adsorption for acid dyes over CeO_2.xH_2O synthesized by a facile method, J. Alloys. Compd. 776 (2019) 96–104, https://doi.org/10.1016/j.jallcom.2018.10.228.
[28] Q. Feng, Z. Zhang, Y. Ma, X. He, Y. Zhao, Z. Chai, Adsorption and desorption characteristics of arsenic onto ceria nanoparticles, Nanoscale Res. Lett. 7 (84) (2012) 1–8 http://www.nanosclaereslett.com/content/7/1/84.
[29] S. Yari, S. Abbasizadeh, S.E. Mousavi, M.S. Moghaddam, A.Z. Moghaddam, Adsorption of Pb(II) and Cu(II) ions from aqueous solution by an electrospun CeO_2 nanofiber adsorbent functionalized with mercapto groups, Process Saf. Environ. Prot. 94 (2015) 159–171, https://doi.org/10.1016/j.psep.2015.01.011.
[30] J. Sun, C. Wang, L. Zeng, P. Xu, X. Yang, J. Chen, X. Xing, Q. Jin, R. Yu, Controllable assembly of CeO_2 micro/nanospheres with adjustable size and their application in Cr(IV) adsorption, Mater. Res. Bull. 75 (2016) 110–114, https://doi.org/10.1016/j.materresbull.2015.11.035.
[31] Ci Z, J. Gan, Y. Xue, J. Zhang, R. Zhang, J. Liu, J. Hao, Adsorption selectivity of cubic nano-CeO_2 and effect of particle size on adsorption thermodynamics, Fluid Ph. Equilibria 502 (2019) 112277, , https://doi.org/10.1016/j.fluid.2019.112277.
[32] S. Mishra, S. Soren, A.K. Debnath, D.K. Aswal, N. Das, P. Parhi, Rapid microwave-hydrothermal synthesis of CeO_2 nanoparticles for simultaneous adsorption/photo-degradation of organic dyes under visible light, Optik 169 (2018) 125–136, https://doi.org/10.1016/j.ijleo.2018.05.045.
[33] M. Brigante, M.P.C. Schulz, Adsorption of the antibiotic minocycline on cerium (IV) oxide: effect of pH, ionic strength and temperature, Microporous Mesoporous Mater. 156 (2012) 138–144 doi:10.106/j.micromeso.2012.02.033..
[34] M. Brigante, M.P.C. Schulz, Cerium (IV) oxide: synthesis in alkaline and acidic media, characterization and adsorption properties, Chem. Eng. J. 191 (2012) 563–570, https://doi.org/10.1016/j.cej.2012.02.064.
[35] N. Zhang, J. Chen, Z. Fang, E.P. Tsang, Ceria accelerated nanoscale zerovalent iron assisted heterogeneous Fenton oxidation of tetracycline, Chem. Eng. J. 369 (2019) 588–599, https://doi.org/10.1016/j.cej.2019.03.112.
[36] T.J. Al-Musawi, F. Brouers, M. Zarrabi, Kinetic modelling of antibiotic adsorption onto different nanomaterials using the Brouers-Sotolongo fractal equation, Environ. Sci. Pollut. Res. 24 (2017) 4048–4057, https://doi.org/10.1007/s11356-016-8182-z.

[37] H.R. Pouretedal, N. Sadegh, Effective removal of Amoxicillin, Cephalexin, Tetracycline and Penicilin G from aqueous solution using activated carbon nanoparticles prepared from vine wood, J. Water Process Eng. 1 (2014) 64–73, https://doi.org/10.1016/j.jwpe.2014.03.006.

[38] M.J. Ahmed, Md. Azharul Islam, M. Asif, B.H. Hameed, Human hair-derived high surface area porous carbon material for the adsorption isotherm and kinetics of tetracycline antibiotics, Bioresour. Technol. 243 (2017) 778–784, https://doi.org/10.1016/j.biortech.2017.06.174.

[39] A. Sheikhmohammadi, M. Safari, A. Alinejad, A. Esrafili, H. Nourmoradi, E. Asgari, The synthesis and application of the $Fe_3O4@SiO_2$nanoparticles functionalized with 3-aminopropyltriethoxysilane as an efficient sorbent for adsorption of ethylparaben from wastewater: Synthesis, kinetic, thermodynamic and equilibrium studies, J. Environ. Chem. Eng. 7 (2019) 103315, , https://doi.org/10.1016/j.jece.2019.103315.

[40] H. Godini, F. Hashemi, L. Mansuri, M. Sardar, G. Hassani, S.M. Mohseni, A.A. Alinejad, S. Golmohammadi, A. Sheikh Mohammadi, Water polishing of phenol by walnut green hull as adsorbent: an insight of adsorption isotherm and kinetic, J. Water Reuse Des. 06 (4) (2016) 544–552, https://doi.org/10.2166/wrd.2016.068.

[41] R. Acosta, V. Fierro, A. Martinez de Yuso, D. Nabarlatz, A. Celzard, Tetracycline adsorption onto activated carbons produced by KOH activation of tyre pyrolysis char, Chemosphere 149 (2016) 168–176, https://doi.org/10.1016/j.chemosphere.2016.01.093.